

Scalable One-Step Assembly of an Inexpensive Photoelectrode for Water Oxidation by Deposition of a Ti- and Ni-Containing Molecular Precursor on Nanostructured WO_3

Yi-Hsuan Lai, Timothy C. King, Dominic S. Wright, and Erwin Reisner*^[a]

Water oxidation is a key challenge to a future energy technology that utilizes solar energy to split water or to reduce carbon dioxide.^[1] Photocatalyzing this demanding four-electron, four-proton process efficiently remains an unresolved task and a topic of much current interest.^[2] A photo- O_2 evolution system requires the efficient combination of light harvesting, multi-charge separation and water-oxidation catalysis; all of which are coupled superbly in natural photosynthesis.^[3]

Although considerable progress was made recently in the assembly of improved water-oxidizing photoanodes,^[4] they typically rely on the use of expensive materials and/or non-scalable fabrication procedures. However, scalable low-cost strategies are required to allow wide adoption of such systems. A promising and emerging approach to form surface-immobilized water-oxidation electrocatalysts is the deposition of molecular precursors on a conducting or semiconducting substrate. For example, Co-containing compounds, as well as a Mn-based molecule, were recently used for the formation of a CoO_x and a Mn-based water-oxidation electrocatalyst in a pH-neutral environment.^[5] We were interested to investigate if this approach could be extended to fabricate an O_2 -evolving photoelectrode by depositing a molecular heterobimetallic precursor on a semiconductor for the simultaneous formation of an electrocatalyst and a stabilizing layer for the substrate.

Herein, we report the assembly of a water-oxidizing photoanode in a straightforward and simple procedure by spin-coating of $[\text{Ti}_2(\text{OEt})_9(\text{NiCl})]_2$ (TiNi) on a nanostructured WO_3 (nanoWO_3) electrode (Figure 1). TiNi serves as a molecular single-source precursor for both NiO_x , which acts as the electrocatalyst, and TiO_2 , which stabilizes the WO_3 semiconductor. The resulting $\text{nanoWO}_3|\text{TiNi}$ electrode contains

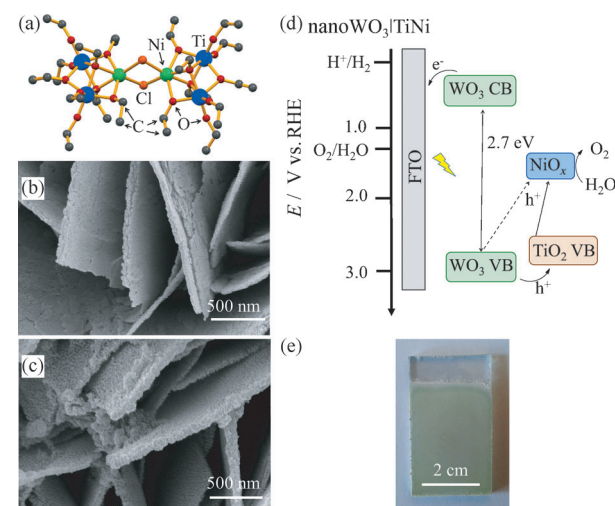


Figure 1. a) Molecular structure of $[\text{Ti}_2(\text{OEt})_9(\text{NiCl})]_2$ (TiNi) based on crystallographic coordinates (hydrogen atoms and disordered ethoxy groups are omitted for clarity).^[7] Ni (green), Ti (blue), Cl (orange), O (red), C (grey). SEM images of b) unmodified nanoWO_3 and c) $\text{nano-WO}_3|\text{TiNi}$. d) Schematic energy diagram for solar-light-driven water oxidation with $\text{nanoWO}_3|\text{TiNi}$. e) Photograph image of $\text{nanoWO}_3|\text{TiNi}$.

solely Earth-abundant materials and photo-oxidizes water to O_2 , with WO_3 acting as the solar-light harvesting semiconductor.^[6] The one-step co-deposition of a protecting layer, such as TiO_2 and water oxidation catalyst, such as NiO_x , is an attractive approach to improve photoelectrochemical (PEC) water oxidation.

The precursor TiNi contains a dimeric $[\text{Ni}(\mu\text{-Cl})_2\text{Ni}]^{2+}$ bridged core with two attached $[\text{Ti}_2(\text{OEt})_9]^-$ moieties (Figure 1 a) and was readily obtained through a solvothermal reaction of $\text{Ti}(\text{OEt})_4$ with NiCl_2 .^[7] We first assessed the hydrolytic decomposition of TiNi into TiO_2 and the electroactivity of NiO_x . A water-oxidizing electrode (FTO|TiNi) was assembled by drop-casting TiNi in toluene (10 μL of a 5 mM solution) on a fluoride-doped tin oxide (FTO)-coated glass substrate with an exposed geometrical surface area of 0.5 cm^2 . Hydrolysis and polycondensation of TiNi gave a mixture of amorphous TiO_2 (Figure S1 in the Supporting Information)^[8] and NiO_x , which was confirmed by energy-dispersive X-ray (EDX) analysis (Ti to Ni ratio of ca. 2 to 1; Table S1 in the Supporting Information) and electrochemical investigations. NiO_x is a known electrocatalyst for water oxidation in borate solution,^[9] and NiO_x on FTO|TiNi elec-

[a] Y.-H. Lai, T. C. King, Prof. D. S. Wright, Dr. E. Reisner
Christian Doppler Laboratory for Sustainable SynGas Chemistry
Department of Chemistry, University of Cambridge
Lensfield Road, Cambridge CB2 1EW (UK)
E-mail: reisner@ch.cam.ac.uk

Supporting information for this article is available on the WWW under <http://dx.doi.org/10.1002/chem.201302641>.

© 2013 The Authors. Published by Wiley-VCH Verlag GmbH & Co. KGaA. This is an open access article under the terms of the Creative Commons Attribution License, which permits use, distribution and reproduction in any medium, provided the original work is properly cited.

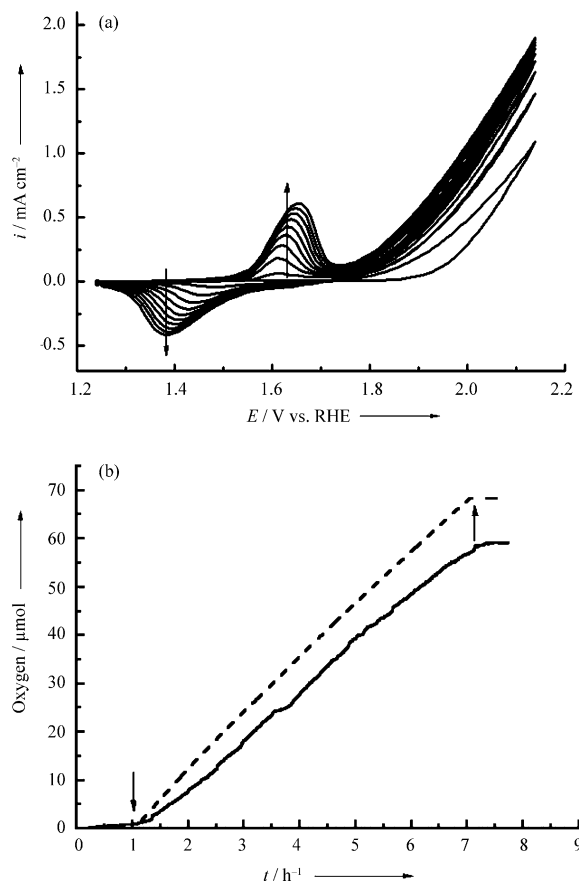


Figure 2. a) Consecutive cyclic voltammograms with FTO|TiNi in an aqueous Bi solution (0.1 M, pH 9.2) at RT and a scan rate of 50 mV s⁻¹ showing the increase in the Ni^{II/III} oxidation wave^[9a,b] at approximately $E_p = 1.62$ V versus RHE and the wave for electrocatalytic water oxidation at an onset potential of approximately $E_{\text{cat}} = 1.73$ V versus RHE. A platinum counter and a Ag/AgCl/KCl(sat) reference electrode were employed. b) Amount of O₂ evolved during controlled potential electrolysis with FTO|TiNi under the same conditions at an applied potential of 2.0 V versus RHE between one and seven hours. The amount of O₂ was quantified by an O₂ fluorescence probe (solid trace) and the dashed trace shows the theoretical amount of O₂ calculated based on 100% Faradaic efficiency.

tro-oxidizes water to O₂ with approximately 90% Faradaic efficiency in potassium borate solution (0.1 M, Bi) at pH 9.2 with a potential of 2.0 V versus the reversible-hydrogen electrode (RHE, Figure 2).

WO₃ is an inexpensive, easily prepared and robust n-type semiconductor with a suitable band structure to absorb visible light (ca. 2.7 eV) and to photo-oxidize water (valence-band potential at ca. 3 V vs. RHE; Figure 1 d).^[6,10] Although the valence band of WO₃ is not negative enough to achieve hydrogen evolution, it can be coupled with a photocathode to accomplish bias-free overall water splitting.^[11] Drawbacks of bare WO₃ are its chemical dissolution at pH > 4,^[12] as well as sluggish catalysis and poor selectivity.^[13] The slow release of O₂ also allows competing side reactions, such as the generation of H₂O₂, to occur, which causes photodegradation of WO₃.^[13a,14] Covering metal oxides with an electrocatalyst and/or protective layer based on transition-metal

oxides is a successful strategy to improve their photoactivity and stability,^[4b,5e,14,15] and we explore covering WO₃ with TiNi to improve its performance.

WO₃ can be prepared by several methods, such as atomic-layer deposition (ALD),^[5e] electrodeposition,^[14] anodization of tungsten foil,^[16] sol-gel synthesis^[17] and hydrothermal synthesis.^[18] We prepared nanoWO₃ by the latter method, because it is suitable to prepare vertically aligned nanostructured WO₃ readily and at a low cost (see the Supporting Information for SEM images and powder XRD patterns; Figures 1b and S2 in the Supporting Information).^[11a,18a] The sheet-like structure enhances the exposed surface area and decreases the hole diffusion length in nanoWO₃. NanoWO₃|TiNi electrodes were prepared by spin coating a toluene solution of TiNi on nanoWO₃. After four cycles ($N=4$), a quantitative surface coverage of the nanoWO₃ sheets with TiNi was obtained (see the Experimental Section, Figures 1c and S3 in the Supporting Information). There was no obvious change in surface morphology of nanoWO₃ after multiple deposition cycles with TiNi, except that the nanoWO₃ was decorated with Ti- and Ni-containing nanoparticles, forming a rough and uniform nanoWO₃|TiNi surface. EDX analyses confirmed a 2:1 to 3:1 stoichiometry of titanium and nickel on the WO₃ surface (Table S1 and Figure S4 in the Supporting Information).

WO₃ electrodes are typically only studied under acidic conditions due to the poor photostability of the semiconductor in a basic environment.^[5e,14,16–18] Previously, a nanostructured WO₃ electrode prepared by ALD was modified with a Mn-based catalyst and displayed activity for photocatalytic water oxidation between pH 4 and 7.^[5e] A planar WO₃ electrode modified with CoO_x was also reported to show high photostability in an aqueous phosphate solution at pH 7.^[14]

We decided to study the enhanced performance of the nanoWO₃|TiNi electrodes in an alkaline environment to demonstrate that coating with TiNi can stabilize WO₃ under such demanding conditions. Our rationale for improved photoactivity and stability of nanoWO₃|TiNi was that TiO₂ would serve as a charge-separation layer for transferring holes from the photoexcited WO₃, thereby decreasing the rate of charge recombination.^[19] In addition, TiO₂ is a known alkaline-resistant material and can at least partly protect WO₃ from direct contact with the basic solution. NiO_x is an active water-oxidation catalyst in basic borate solution (see above),^[9] and should act as the electro-catalyst driven by photogenerated holes from the valence band of WO₃. We note that at least some NiO_x is likely to be in close contact with WO₃, and hole transfer is therefore also possible to NiO_x directly from WO₃ (Figure 1d).

Photocurrents were measured in a three-electrode configuration with a platinum foil counterelectrode and a Ag/AgCl/KCl(sat) reference electrode at RT, using standardized solar-light irradiation (AM 1.5G, 100 mW cm⁻²). In pH 9.2 Bi solution (0.1 M) at an applied potential of 0.94 and 1.23 V versus RHE, bare nanoWO₃ showed an initial photocurrent of 131 and 430 $\mu\text{A cm}^{-2}$ with 28 ± 1 and 10 ± 2 % of the photocurrent remaining after 1 h, respectively (Figure 3). An in-

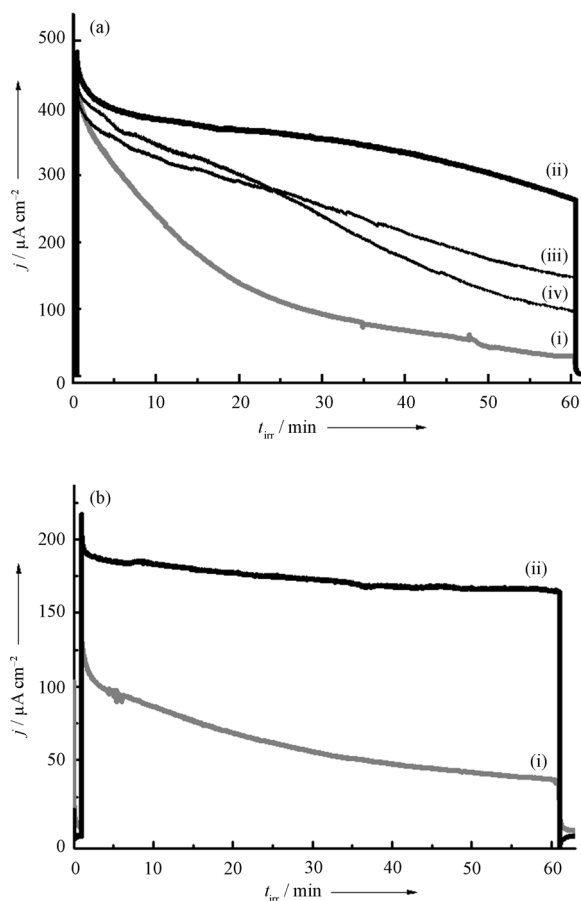


Figure 3. Chronoamperometric measurements a) at 1.23 and b) 0.94 V versus RHE in a pH 9.2 Bi buffer. Photocurrent profiles of i) nanoWO₃, ii) nanoWO₃|TiNi, iii) nanoWO₃|Ni(NO₃)₂ and iv) nanoWO₃|[Ti(OiPr)₄] under standardized solar-light irradiation (AM 1.5 G, 100 mW cm⁻²) are shown.

creasing number of TiNi deposition cycles (N) resulted in enhanced photostability with 73 ± 3 and 58 ± 3 % of the photocurrent remaining after 1 h continuous irradiation with $N=4$ at 0.94 and 1.23 V versus RHE, respectively (Figures 3 and S5–S6 in the Supporting Information). A half-life time of more than 4 h was found at an applied potential of 0.94 V versus RHE in pH 9.2 Bi solution in the case of nanoWO₃|TiNi (Figure S7 in the Supporting Information), whereas nanoWO₃ had lost 50 % of its photoactivity after 35 min. Control experiments involving spin coating Ni(NO₃)₂ in 2-methoxyethanol (nanoWO₃|Ni(NO₃)₂, 30 μL , 10 mM) and titanium isopropoxide, [Ti(OiPr)₄] in toluene (30 μL , 20 mM) on nanoWO₃ (nanoWO₃|[Ti(OiPr)₄]) resulted in stabilities between those for bare nanoWO₃ and nanoWO₃|TiNi electrodes. This observation demonstrates that NiO_x acts as an electrocatalyst and TiO₂ provides a protective layer (Figures 3a and S5 in the Supporting Information). The same general trend was also observed in a pH 8.2 Bi electrolyte solution (Figure S8 in the Supporting Information).

The amount of O₂ and H₂ (from the platinum counterelectrode in an air-tight three-electrode two-compartment cell) liberated into the headspace of the anodic and cathodic

compartments during irradiation was measured by using a fluorescence O₂ sensor and gas chromatography, respectively (see the Supporting Information, Table S2 and Figure S9). An average charge of 1.17 ± 0.16 and 0.49 ± 0.05 C cm⁻² h⁻¹ was passed through the nanoWO₃|TiNi and nanoWO₃ electrodes, respectively, after 1 h irradiation at pH 9.2 and 1.23 V versus RHE. The corresponding Faradaic efficiencies for O₂ evolution were 74 ± 3 % (with 2.2 ± 0.3 μmol O₂ cm⁻² h⁻¹) for nanoWO₃|TiNi and 56 ± 2 % (with 0.71 ± 0.06 μmol O₂ cm⁻² h⁻¹) for bare nanoWO₃. Comparable Faradaic yields of 78 ± 1 % (4.70 ± 0.65 μmol H₂ cm⁻² h⁻¹) and 77 ± 2 % (1.94 ± 0.28 μmol H₂ cm⁻² h⁻¹) were obtained for H₂ evolution on the platinum counterelectrode by using nanoWO₃|TiNi and nanoWO₃, respectively. The H₂/O₂ ratio is therefore close to 2:1 for the nanoWO₃|TiNi system, whereas it is larger than the ideal 2:1 ratio by using bare nanoWO₃. The decreased charge generated by bare nanoWO₃ presumably stems from its poor stability in basic Bi solution, which also results in non-stoichiometric O₂ evolution and suggests that a considerable portion of the photo-generated holes are used for side reactions. This limitation is largely offset by nanoWO₃|TiNi. Based on the amount of O₂ evolution and TiNi on the surface of nanoWO₃, the turnover frequency of NiO_x is approximately 8×10^{-4} s⁻¹ at 1.23 V versus RHE (see the Supporting Information).

Studying the photocurrents of the nanoWO₃ electrodes at different potentials at pH 9.2 provided a more comprehensive understanding of the TiNi modification, in particular of the efficiency for photo-water oxidation at a low over-potential. The bare nanoWO₃ electrode showed an onset photocurrent at 0.74 V versus RHE and the photocurrent increases by applying a more positive potential (Figure 4a, trace i). The photocurrent saturates at approximately $500 \mu\text{A cm}^{-2}$ at 1.34 V versus RHE.

Modification of nanoWO₃ with TiNi resulted in an approximately 100 mV cathodic shift of the onset potential (Figure 4a, trace ii). The effect of the TiNi deposition is particularly evident from enhanced anodic photocurrents in the low bias region (<1.15 V vs. RHE). For example, $107 \pm 2 \mu\text{A cm}^{-2}$ was obtained with nanoWO₃|TiNi at 0.84 V vs. RHE, whereas only $41 \pm 5 \mu\text{A cm}^{-2}$ was observed with bare nanoWO₃ at the same potential. A decreased charge-transfer resistance with nanoWO₃|TiNi was also confirmed by electrochemical impedance spectroscopy at this potential (Figure 4b). A significant contribution from UV band-gap excitation of TiO₂ to the total photocurrent density with nanoWO₃|TiNi can be ruled out, because a comparable photocurrent enhancement was observed both in the presence and absence of a 420 nm UV cut-off filter with nanoWO₃|TiNi and unmodified WO₃. A significant enhancement in photocurrent was also observed when modifying nanoWO₃ with [Ti(OiPr)₄] in the presence of 420 nm cut-off filter at 0.84 V versus RHE, suggesting that TiO₂ improves charge separation on the photoanode.

In summary, a nanoWO₃|TiNi electrode, which is readily prepared from inexpensive materials by using a simple single-source approach, was reported. This technique allows

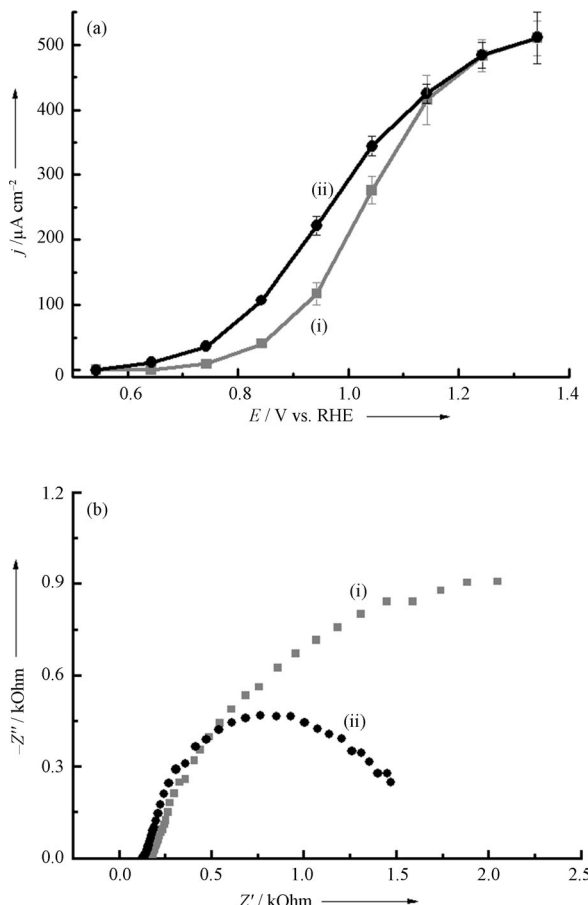


Figure 4. a) Photocurrent responses at various potentials and b) the Nyquist plots at an applied potential of 0.84 V versus RHE of i) an unmodified nanoWO_3 electrode and ii) a $\text{nanoWO}_3|\text{TiNi}$ electrode under standardized solar-light irradiation (AM 1.5 G, 100 mW cm^{-2}) in an aqueous Bi solution (0.1 M, pH 9.2).

coating of a semiconductor substrate with an electrocatalyst and a stabilizing layer by using a homogeneous, heterobimetallic precursor in one-step. The $\text{nanoWO}_3|\text{TiNi}$ electrode showed enhanced water-oxidation catalysis, suffers from fewer limitations from charge recombination than unmodified nanoWO_3 and allows for the employment of WO_3 under basic conditions. Our approach can be widely applied to other nanostructured semiconductors and redox reactions. Work is currently in progress in exploring other single-source precursors on different semiconductors to produce new photoactive nanocomposite materials.

Experimental Section

Preparation of FTO|TiNi electrode: The water-oxidation electrode was prepared by drop-casting fresh solutions of TiNi (10 μL of 5 mM in toluene) on fluoride-doped tin oxide (FTO; Pilkington; TEC Glass 7; sheet resistance 7 Ohm sq^{-1}) coated glass (exposed surface area of 0.5 cm^2 controlled by 1350F polyester tape, 3 M). The FTO|TiNi electrode was left at least for 30 min in air at RT, whereupon the electrode was rinsed with water.

Preparation of $\text{nanoWO}_3|\text{TiNi}$ electrode: The water-oxidation photoelectrode was prepared by spin coating a fresh solution of TiNi (30 μL of 5 mM in toluene) on nanoWO_3 (exposed area: 0.5 cm^2) at 2000 rpm for 10 s. This procedure was repeated N times. The $\text{nanoWO}_3|\text{TiNi}$ electrode was dried for at least 30 min in air at RT and then washed with water prior to use. For comparison, $\text{nanoWO}_3|\text{Ni}(\text{NO}_3)_2$ and $\text{nanoWO}_3|\text{[Ti(OiPr)}_4]$ were prepared by spin coating nickel(II) nitrate hexahydrate ($\text{Ni}(\text{NO}_3)_2 \cdot 6 \text{ H}_2\text{O}$, 30 μL of 10 mM in 2-methoxyethanol; BDH Chemical) and a titanium isopropoxide solution ($[\text{Ti(OiPr)}_4]$, 30 μL of 20 mM in toluene; 97%; Sigma-Aldrich) on nanoWO_3 according to the same procedure.

Electrochemical and PEC measurements: An Ivium CompactStat potentiostat by using a conventional three-electrode system was employed. FTO|TiNi, nanoWO_3 , $\text{nanoWO}_3|\text{TiNi}$, $\text{nanoWO}_3|\text{Ni}(\text{NO}_3)_2$ and $\text{nanoWO}_3|\text{[Ti(OiPr)}_4]$ were used as the working electrodes (all with exposed area of 0.5 cm^2). A Ag/AgCl/KCl(sat) electrode was used as the reference electrode, and a platinum foil as the counterelectrode. All electrode systems were measured at RT in an aqueous potassium borate solution (Bi, pH 9.2 or pH 8.2). The potentials were converted to the reversible hydrogen electrode (RHE) by using the following Equation:

$$E (\text{V vs. RHE}) = E (\text{V vs. Ag/AgCl}) + 0.197 + 0.059 \times \text{pH}^{[20]}$$

A solar-light simulator (Newport Oriel, 150 W) was used as a light source. The light intensity was adjusted to 100 mW cm^{-2} (1 sun), and an air mass 1.5 global filter and an IR water filter were used.

Detection and quantification of O_2 and H_2 : Electrochemical and PEC water oxidation were carried out by using an electrochemical cell with two compartments separated by a film of Nafion. Headspace O_2 and H_2 were quantified by using an Ocean Optics fluorescence oxygen probe (FOXY-R) and/or a gas chromatograph. A potential of 2.0 V versus RHE (no compensation for iR drop) was applied for electrocatalytic water oxidation, whereas a potential of 1.23 V versus RHE for PEC water oxidation. Note that the total amount of O_2 evolved was determined as the sum of O_2 measured in the headspace by using the ideal-gas law plus dissolved O_2 in the solution calculated by Henry's Law. Please see the Supporting Information for more detailed descriptions.

Acknowledgements

Financial support from EPSRC (EP/H00338X/2), the Christian Doppler Research Association (Austrian Federal Ministry of Economy, Family and Youth and National Foundation for Research, Technology and Development) and the OMV Group (all to E.R.) is gratefully acknowledged. We also thank the Government scholarship to Study Abroad by the Ministry of Education of Taiwan (SAS-100-1-13-2-UK-034) and the Cambridge Trust (both to Y.H.L.). T.C.K. was supported by EPSRC. We also thank Mr. Yaokang Lv for initial help in the synthetic part of the work and Mr. Dirk Mersch for recording SEM images and measuring EDX.

Keywords: photochemistry • photooxidation • photosynthesis • water oxidation • water splitting

- [1] a) J. Wang, H.-X. Zhong, Y.-L. Qin, X.-B. Zhang, *Angew. Chem.* **2013**, *125*, 5356–5361; *Angew. Chem. Int. Ed.* **2013**, *52*, 5248–5253;
- b) Y. Tachibana, L. Vayssières, J. R. Durrant, *Nat. Photonics* **2012**, *6*, 511–518; c) Y. Jiang, F. Li, B. Zhang, X. Li, X. Wang, F. Huang, L. Sun, *Angew. Chem.* **2013**, *125*, 3482–3485; *Angew. Chem. Int. Ed.* **2013**, *52*, 3398–3401; d) R. D. L. Smith, M. S. Prévôt, R. D. Fagan, Z. Zhang, P. A. Sedach, M. K. J. Siu, S. Trudel, C. P. Berlinguet, *Science* **2013**, *340*, 60–63; e) S. Y. Reece, J. A. Hamel, K. Sung, T. D. Jarvi, A. J. Esswein, J. J. H. Pijpers, D. G. Nocera, *Science* **2011**, *334*, 645–648; f) C.-Y. Lee, K. Lee, P. Schmuki, *Angew. Chem.* **2013**, *125*,

- 2131–2135; *Angew. Chem. Int. Ed.* **2013**, *52*, 2077–2081; g) F. Lakadamyali, M. Kato, N. M. Muresan, E. Reisner, *Angew. Chem.* **2012**, *124*, 9515–9518; *Angew. Chem. Int. Ed.* **2012**, *51*, 9381–9384.
- [2] a) G. Chen, L. Chen, S.-M. Ng, W.-L. Man, T.-C. Lau, *Angew. Chem.* **2013**, *125*, 1833–1835; *Angew. Chem. Int. Ed.* **2013**, *52*, 1789–1791; b) M. Barroso, C. A. Mesa, S. R. Pendlebury, A. J. Cowan, T. Hisatomi, K. Sivula, M. Grätzel, D. R. Klug, J. R. Durrant, *Proc. Natl. Acad. Sci. USA* **2012**, *109*, 15640–15645; c) J. Brillet, J.-H. Yum, M. Cornuz, T. Hisatomi, R. Solarzka, J. Augustynski, M. Grätzel, K. Sivula, *Nat. Photonics* **2012**, *6*, 824–828.
- [3] a) K. N. Ferreira, T. M. Iverson, K. Maghlaoui, J. Barber, S. Iwata, *Science* **2004**, *303*, 1831–1838; b) H. Dau, I. Zaharieva, *Acc. Chem. Res.* **2009**, *42*, 1861–1870; c) Y. Umena, K. Kawakami, J.-R. Shen, N. Kamiya, *Nature* **2011**, *473*, 55–60; d) M. Kato, T. Cardona, A. W. Rutherford, E. Reisner, *J. Am. Chem. Soc.* **2012**, *134*, 8332–8335.
- [4] a) C. Liu, J. Tang, H. M. Chen, B. Liu, P. Yang, *Nano Lett.* **2013**, *13*, 2989–2992; b) S. D. Tilley, M. Cornuz, K. Sivula, M. Grätzel, *Angew. Chem.* **2010**, *122*, 6549–6552; *Angew. Chem. Int. Ed.* **2010**, *49*, 6405–6408; c) W. J. Youngblood, S. H. A. Lee, Y. Kobayashi, E. A. Hernandez-Pagan, P. G. Hoertz, T. A. Moore, A. L. Moore, D. Gust, T. E. Mallouk, *J. Am. Chem. Soc.* **2009**, *131*, 926–927; d) Y. Gao, X. Ding, J. Liu, L. Wang, Z. Lu, L. Li, L. Sun, *J. Am. Chem. Soc.* **2013**, *135*, 4219–4222.
- [5] a) Y.-H. Lai, C.-Y. Lin, Y. Lv, T. C. King, A. Steiner, N. M. Muresan, L. Gan, D. S. Wright, E. Reisner, *Chem. Commun.* **2013**, *49*, 4331–4333; b) J. J. Stracke, R. G. Finke, *J. Am. Chem. Soc.* **2011**, *133*, 14872–14875; c) S. Cobo, J. Heidkamp, P. A. Jacques, J. Fize, V. Fourmond, L. Guetaz, B. Jousseline, V. Ivanova, H. Dau, S. Palacin, M. Fontecave, V. Artero, *Nat. Mater.* **2012**, *11*, 802–807; d) A. Han, H. Wu, Z. Sun, H. Jia, P. Du, *Phys. Chem. Chem. Phys.* **2013**, *15*, 12534–12538; e) R. Liu, Y. Lin, L.-Y. Chou, S. W. Sheehan, W. He, F. Zhang, H. J. M. Hou, D. Wang, *Angew. Chem.* **2011**, *123*, 519–522; *Angew. Chem. Int. Ed.* **2011**, *50*, 499–502.
- [6] C. A. Bignozzi, S. Caramori, V. Cristino, R. Argazzi, L. Meda, A. Tacca, *Chem. Soc. Rev.* **2013**, *42*, 2228–2246.
- [7] S. Eslava, M. McPartlin, R. I. Thomson, J. M. Rawson, D. S. Wright, *Inorg. Chem.* **2010**, *49*, 11532–11540.
- [8] a) H.-S. Chen, R. V. Kumar, *RSC Adv.* **2012**, *2*, 2294–2301; b) X. Chen, S. S. Mao, *Chem. Rev.* **2007**, *107*, 2891–2959.
- [9] a) M. Dincă, Y. Surendranath, D. G. Nocera, *Proc. Natl. Acad. Sci. USA* **2010**, *107*, 10337–10341; b) A. Singh, S. L. Y. Chang, R. K. Hocking, U. Bach, L. Spiccia, *Energy Environ. Sci.* **2013**, *6*, 579–586; c) D. K. Bediako, Y. Surendranath, D. G. Nocera, *J. Am. Chem. Soc.* **2013**, *135*, 3662–3674; d) M. Risch, K. Klingan, J. Heidkamp, D. Ehrenberg, P. Chernev, I. Zaharieva, H. Dau, *Chem. Commun.* **2011**, *47*, 11912–11914.
- [10] a) G. Hodes, D. Cahen, J. Manassen, *Nature* **1976**, *260*, 312–313; b) T. Bak, J. Nowotny, M. Rekas, C. C. Sorrell, *Int. J. Hydrogen Energy* **2002**, *27*, 991–1022; c) C. Santato, M. Odziedkowski, M. Ulmann, J. Augustynski, *J. Am. Chem. Soc.* **2001**, *123*, 10639–10649; d) Z. Chen, T. F. Jaramillo, T. G. Deutsch, A. Kleiman-Shwarzstein, A. J. Forman, N. Gaillard, R. Garland, K. Takanabe, C. Heske, M. Sunkara, E. W. McFarland, K. Domen, E. L. Miller, J. A. Turner, H. N. Dinh, *J. Mater. Res.* **2010**, *25*, 3–16.
- [11] a) C.-Y. Lin, Y.-H. Lai, D. Mersch, E. Reisner, *Chem. Sci.* **2012**, *3*, 3482–3487; b) H. Wang, T. Deutsch, J. A. Turner, *J. Electrochem. Soc.* **2008**, *155*, F91–F96.
- [12] R. S. Lillard, G. S. Kanner, D. P. Butt, *J. Electrochem. Soc.* **1998**, *145*, 2718–2725.
- [13] a) J. C. Hill, K. S. Choi, *J. Phys. Chem. C* **2012**, *116*, 7612–7620; b) Q. Mi, A. Zhanaidarov, B. S. Brunschwig, H. B. Gray, N. S. Lewis, *Energy Environ. Sci.* **2012**, *5*, 5694–5700.
- [14] J. A. Seabold, K. S. Choi, *Chem. Mater.* **2011**, *23*, 1105–1112.
- [15] a) S. S. K. Ma, K. Maeda, R. Abe, K. Domen, *Energy Environ. Sci.* **2012**, *5*, 8390–8397; b) D. K. Zhong, D. R. Gamelin, *J. Am. Chem. Soc.* **2010**, *132*, 4202–4207; c) B. Klahr, S. Gimenez, F. Fabregat-Santiago, J. Bisquert, T. W. Hamann, *J. Am. Chem. Soc.* **2012**, *134*, 16693–16700.
- [16] a) N. R. de Tacconi, C. R. Chenthamarakshan, G. Yogeeshwaran, A. Watcharenwong, R. S. de Zoysa, N. A. Basit, K. Rajeshwar, *J. Phys. Chem. B* **2006**, *110*, 25347–25355; b) V. Cristino, S. Caramori, R. Argazzi, L. Meda, G. L. Marra, C. A. Bignozzi, *Langmuir* **2011**, *27*, 7276–7284; c) A. Tacca, L. Meda, G. Marra, A. Savoini, S. Caramori, V. Cristino, C. A. Bignozzi, V. G. Pedro, P. P. Boix, S. Gimenez, J. Bisquert, *ChemPhysChem* **2012**, *13*, 3025–3034.
- [17] a) J. K. Kim, K. Shin, S. M. Cho, T. W. Lee, J. H. Park, *Energy Environ. Sci.* **2011**, *4*, 1465–1470; b) L. Meda, G. Tozzola, A. Tacca, G. Marra, S. Caramori, V. Cristino, C. A. Bignozzi, *Sol. Energy Mater. Sol. Cells* **2010**, *94*, 788–796.
- [18] a) J. Su, X. Feng, J. D. Sloppy, L. Guo, C. A. Grimes, *Nano Lett.* **2011**, *11*, 203–208; b) S. S. Kalanur, Y. J. Hwang, S. Y. Chae, O. S. Joo, *J. Mater. Chem. A* **2013**, *1*, 3479–3488; c) G. Wang, Y. Ling, H. Wang, X. Yang, C. Wang, J. Z. Zhang, Y. Li, *Energy Environ. Sci.* **2012**, *5*, 6180–6187; d) J. Yang, W. Li, J. Li, D. Sun, Q. Chen, *J. Mater. Chem.* **2012**, *22*, 17744–17752.
- [19] a) I. Shiyanovskaya, M. Hepel, *J. Electrochem. Soc.* **1999**, *146*, 243–249; b) D. Y. C. Leung, X. Fu, C. Wang, M. Ni, M. K. H. Leung, X. Wang, X. Fu, *ChemSusChem* **2010**, *3*, 681–694.
- [20] A. Kay, I. Cesar, M. Grätzel, *J. Am. Chem. Soc.* **2006**, *128*, 15714–15721.

Received: July 8, 2013

Published online: August 14, 2013